

# Environmental impact evaluation and long-term rutting resistance performance of warm mix asphalt technologies

Shenghua Wu<sup>a,\*</sup>, Omar Tahri<sup>a</sup>, Shihui Shen<sup>b</sup>, Weiguang Zhang<sup>c</sup>, Balasingam Muhunthan<sup>d</sup>

<sup>a</sup> Department of Civil, Coastal, and Environmental Engineering, University of South Alabama, 150 Student Services Drive, Shelby Hall 3116, Mobile, AL, 36688, USA

<sup>b</sup> Rail Transportation Engineering, Pennsylvania State University, 216E Penn Building, Penn State Altoona, PA, 16601, USA

<sup>c</sup> School of Transportation Engineering, Southeast University, No. 2 Si Pai Lou, Nanjing, 210096, China

<sup>d</sup> Department of Civil and Environmental Engineering, Washington State University, 405 Spokane Street, Sloan 101, Pullman, WA, 99164, USA

## ARTICLE INFO

### Article history:

Received 16 March 2020

Received in revised form

23 July 2020

Accepted 24 August 2020

Available online 30 August 2020

Handling editor: Cecilia Maria Villas Bôas de Almeida

### Keywords:

Warm mix asphalt

Hot mix asphalt

Environmental impacts

CO<sub>2</sub> reduction

Rutting resistance

Field aging

## ABSTRACT

The adoption of warm mix asphalt (WMA) technologies is well accepted due to its promising environmental benefits, however, their long-term field performance is not well understood. This study focused on the long-term rutting resistance of WMA and their companion hot mix asphalt (HMA) based on 83 field samples collected from 28 field projects across the United States covering four climate zones, and quantified environmental impacts for various WMA technologies as compared to HMA. Field cores were evaluated by dynamic modulus, creep compliance, and Hamburg wheel-tracking device tests. Asphalt binders extracted from field cores were evaluated by continuous performance grading (PG), multiple stress creep recovery (MSCR), and monotonic shear tests. The results showed that WMA binders exhibited similar rutting resistance compared with the HMA binders after long-term field aging. Existence of polymer in the asphalt binder was displayed through the plot of non-recoverable creep compliance and percent recovery. The long-term field aged polymer modified asphalt binders for WMA and HMA were comparable. The results also showed that the CO<sub>2</sub> reduction by using WMA ranged from 89.09% to 42.79% depending on WMA type. On average, the CO<sub>2</sub> emission was reduced to 66.89% by using WMA technologies. Overall, environmental impact analysis and long-term field performance results validated the confident use of WMA technologies.

© 2020 Elsevier Ltd. All rights reserved.

## 1. Introduction

Originally from Europe, warm mix asphalt (WMA) technologies have been adopted in the United States for decades, due to its promising environmental benefits as a result of reduced mixing and compaction temperature. To achieve a lower production temperature, there are three categories of WMA technologies: wax additive, chemical additives, and foaming in the form of either water based or water-containing technology (Shen et al., 2017). As a cleaner production of asphalt pavement, applying WMA technologies can reduce the environmental impact by about 33% as compared to conventional hot mix asphalt (HMA) (Blankendaal et al., 2014). There are many approaches to quantify the environmental impacts

of asphalt pavement using WMA, such as hybrid life cycle analysis (Tatari et al., 2012), and heat energy and fuel calculation (Hamzah et al., 2010). Besides the assessment of sustainability of WMA technologies, there still exists a gap in understanding the long-term performance of WMA technologies as compared to conventional HMA.

Regardless of WMA and HMA pavements, the asphalt pavement performance is deteriorated due to the change of asphalt binder over time. While asphalt binder accounts for a small amount, generally 5–7% by weight of asphalt mixture, the selection of asphalt binder has to consider many factors such as local climate, traffic volume, and whether rheological properties of selected asphalt binders can reflect long-term field performance (Wu, 2018; Wu et al., 2019). One of the significant rheological properties of asphalt binder is its ability to resist permanent shearing deformation under traffic loading and to recover during resting period. Many efforts have been devoted to understand the relationship

\* Corresponding author.

E-mail address: [shenghuawu@southalabama.edu](mailto:shenghuawu@southalabama.edu) (S. Wu).

between asphalt binder and asphalt mixture with respect to rutting resistance (Shenoy et al., 2003; Soleymani et al., 2004). However, with green asphalt technologies such as WMA and various recycled materials and modifiers used in asphalt pavement, characterization of asphalt binder has become complex and challenging. Particularly, there exists a gap in understanding how field long-term performance of asphalt binder is aligned to that of asphalt mixture and ultimately pavement performance.

Currently, the selection of asphalt binder is based on Superpave specification that addresses climate condition and traffic volume specific to a project location (Ramadan et al., 2019). The rutting parameter ( $G^*/\sin\delta$ ) has been widely used to determine high temperature performance grade (PG), however, it has been reported to not characterize polymer modified binders adequately (Dongré et al., 2004). Multiple stress creep recovery (MSCR) test was developed to capture non-recoverable creep compliance ( $J_{nr}$ ) and percent recovery (R) especially beneficial for modified asphalt binder (D'Angelo et al., 2007; Behnood et al., 2016). Rutting performance of asphalt mixtures are commonly evaluated by Hamburg wheel tracking device (HWTDD) test, asphalt pavement analyzer (APA), and asphalt mixture performance tester (AMPT). The first two tests produce results of rut depth and number of wheel passes, and the AMPT gives flow number that is the number of compressive loading cycles when the test specimen exhibits shear tertiary flow, all of which are destructive to test specimens. Non-destructive tests may also characterize mixtures' resistance to deformation such as stiffness and creep compliance at high temperature and low loading frequency or longer loading time.

Several studies investigated the correlation between binder properties and mixtures' performance. Domingos et al. (2017) found that the correlation between  $G^*/\sin\delta$  of asphalt binder and flow number of asphalt mixture was inconclusive, whereas ranking of binders and mixtures based on  $J_{nr}$  and flow number was similar. Based on 21 different binders in Arizona, Ramadan et al. (2019) compared  $G^*/\sin\delta$  and  $J_{nr}$  parameters of binders with HWTDD test and repeated load permanent deformation tests of asphalt mixtures and concluded that  $J_{nr}$  related better to mixture rutting than does  $G^*/\sin\delta$ . The mentioned above studies that addressed correlation of asphalt binder and asphalt mixture were based on laboratory-prepared specimens with regional and local asphalt binder types and mixture compositions.

Most performance evaluations were conducted based on laboratory prepared specimens without considering field aging conditions (Gandhi et al., 2009; Behnood et al., 2016). Although rolling thin film oven and pressure aging vessel can be used to simulate short-term and long-term aging of asphalt binder in laboratory, they appear not to capture realistic and complex aging effect in the field as a result of oxidation, ultraviolet light, and long-term period (Kim et al., 2017). Moreover, without a relatively larger sample set, it is less feasible to make a conclusive statement on the direct relationship between asphalt binder and mixture with respect to permanent deformation resistance. Therefore, this paper aims to addressing these issues.

## 2. Objectives

The primary objective of this study is to provide an extensive characterization on long-term field aging on various asphalt binders and mixtures' permanent deformation resistance at high temperatures, as well as to quantify the environmental impacts reduced by various WMA technologies as compared to conventional HMA. The study included 28 field projects using different WMA technologies across the United States that consisted of 83 field samples in a wide ranges of material compositions. The asphalt binders were extracted and recovered from field cores,

which were evaluated by PG, MSCR, and monotonic shear tests. Their corresponding asphalt mixtures' properties were also evaluated by field cores' dynamic modulus, creep compliance, and Hamburg wheel-tracking device test. The correlations between asphalt binders and mixtures with respect to permanent deformation resistance were explored.

## 3. Research methodology

### 3.1. Project description and material collections

The identified 28 field projects were parts of study from NCHRP 9–49A project, as shown in Fig. 1. The project sites were located in four climatic zones: 10 projects in Wet Freeze, 8 in Wet No-Freeze, 6 in Dry Freeze, and 4 in Dry No-Freeze. Each project had a 200-foot (61-meter) HMA control section and several different 200-foot (61-meter) WMA sections. For each section, two types of field cores were extracted: 100-mm and 150-mm in diameter. The 100-mm cores were used for characterizing dynamic modulus and creep compliance, while the 150-mm cores were used for Hamburg wheel-tracking test. All field cores were taken at the non-wheel path to avoid vehicle damage. At least four 150-mm field cores and thirteen 100-mm field cores were acquired for each material type.

Table 1 provides a list of project and material information collected for this study. The investigated WMA types included organic additive (Sasobit), chemicals (Evotherm, Rediset), water-containing additive (Aspha-min, Advera), and water-based foaming (Astec DBG, LEA, Aquablack, Cecabase, and Gencor). The use of WMA is intended to reduce mixing and compaction temperature, and the extent of such temperature reduction is WMA type dependent. A total of 83 material types were studied. Out of 28 projects, 19 projects used polymer-modified binders and 16 projects used reclaimed asphalt pavement (RAP). PG 70-22 binder was most widely used, followed by PG 64–22 and PG 64–28. PG 76-XX binders were typically used to address warm climate and high truck traffic level such as projects in VA I-66 and LA US 61. More details regarding project and mixture information can be found elsewhere (Shen et al., 2017).

### 3.2. Effect of WMA technologies on the production of CO<sub>2</sub>

Fig. 2 illustrates the in-situ construction environment for an overlay project in Tennessee state utilizing HMA and WMA. Less fume was observed during WMA pavement construction (Fig. 2b) than during HMA pavement construction (Fig. 2a), which



Fig. 1. Field projects monitored in this study (Wu et al., 2019).

**Table 1**  
Project and material information.

Climate Zone	Age, Year <sup>1</sup>	Project	Asphalt Binder	Types <sup>3</sup>	Polymer	RAP	
Wet Freeze	2.0	VA I-66	76–22	HMA, Astec DBG	Yes	0%	
	2.1	IL 147	64–22	HMA, Astec DBG	No	10%	
	2.2	MN TH 169	58–28	HMA, Evotherm 3G	No	NA	
	3.0	PA SR 2012	64–22	HMA, LEA, Gencor	No	0%	
	3.2	PA SR 2006	64–22	HMA, Sasobit, Advera	No	0%	
	3.3	IA US 34	58–28	HMA, Sasobit, Evotherm 3G	No	17%	
	5.0	MO Rte. CC	70–22	HMA, Evotherm DAT	Yes	20%	
	5.8	OH SR 541	70–22	HMA, Sasobit, Evotherm ET, Aspha-min	Yes	15%	
	6.2	MO Hall St.	70–22	HMA, Sasobit, Evotherm ET, Aspha-min	Yes	10%	
	6.8	MD 925	70–22	HMA, Sasobit	Yes	15%	
Wet No- Freeze	2.8	LA US 61	76–22	HMA, Sasobit, Evotherm 3G	Yes	15%	
	3.2	TN SR 125	70–22	HMA, Evotherm 3G	Yes	10%	
	3.2	LA 116	70–22	HMA, Foam	Yes	15%	
	4.0	TX FM324	64–22	HMA, Sasobit, Evotherm DAT, Rediset, Advera	Yes	0%	
	4.2	LA 3121	70–22	HMA, Evotherm 3G	Yes	15%	
	4.6	LA 3191	70–22	HMA, Foam	Yes	15%	
	4.8	SC US 178	64–22	HMA, Evotherm DAT	No	NA	
	4.8	TN SR 46	70–22	HMA, Sasobit, Evotherm DAT, Advera, DBG	Yes	0%	
	Dry Freeze	1.7	WA SR 12	64–28	HMA, Aquablack	Yes	20%
		1.8	NV	64–28	HMA, Foam	Yes	15%
1.9		MT I-15	70–28	HMA, Sasobit, Evotherm DAT, Foam	Yes	0%	
4.0		NE US 14a	64–28	HMA, Evotherm	Yes	<15%	
4.0		NE US 14b	64–28	HMA, Advera	Yes	<15%	
4.2		WA I-90	76–28	HMA, Sasobit	Yes	15–20%	
5.3		CO IH 70	58–28	HMA, Sasobit, Evotherm DAT, Advera	No	0%	
Dry No- Freeze		4.3	TX SH 251	70–22	HMA, Astec DBG	Yes	0%
		NA	TX SH 71	76–22	HMA, Evotherm DAT	Yes	NA
		<1	CA HVS 3a <sup>2</sup>	64–16	HMA, Gencor, Evotherm DAT, Cecabase	No	0%
	<1	CA HVS 3b	64–16	HMA, Sasobit, Advera, Astec DBG, Rediset	No	0%	

Note.

1. Age year is counted from construction date to the date when field cores were extracted.
2. CA HVS 3a and 3b projects are based on accelerated pavement facility in California, whose age years are less than 1 year.
3. DBG – double barrel green, LEA – low emission asphalt, DAT – dispersed asphalt technology, NA – not available.

demonstrated that WMA pavement offered a more pleasant working environment for on-site workers (Wu et al., 2017).

To quantify the environmental impact during asphalt mixture production, a heat energy and CO<sub>2</sub> emission approach is used. The heat energy needed to heat the binder and aggregates is calculated as follows (Hamzah et al., 2010):

$$Q = \sum_{i=1}^{j=n-1} mc\Delta\theta \quad (1)$$

where Q is the sum of the heat energy (J), m is the mass of the material (kg), c is the specific heat capacity (J/(kg/°C)), Δθ is the difference between the ambient and mixing temperatures (°C), and i and j are different material types.

Specific heat capacity includes aggregate and asphalt binder.

The specific heat capacity of aggregate can be determined as follows (Waples and Waples, 2004):

$$C_{pnt} = 8.95 \times 10^{-10} T^3 - 2.13 \times 10^{-6} T^2 + 0.00172T + 0.176 \quad (2)$$

$$C^* = \int_{t_i}^{t_j} C_{pnt} dt \quad (3)$$

where T is the temperature (°C), C<sub>pnt</sub> represents the unitless specific heat capacity of the aggregate at the target production temperature, C\* is the specific heat capacity for initial temperature (t<sub>i</sub>) to target production temperature (t<sub>j</sub>), with unit of J/kg/°C.

The initial temperature (t<sub>i</sub>) was assumed to be 25 °C and t<sub>j</sub> represented the temperature of production for each mixture type in



**Fig. 2.** In-situ construction environment: (a) HMA produced at 155–168 °C and (b) WMA-Evothem 3G produced at 135–143 °C (Wu et al., 2017).

(°C). An absolute value of 1 kg was chosen for the mass of the material for both binder and aggregate. The heat energy for binder and aggregate were determined after the specific heat capacity for the selected temperature was calculated following Equation (1). To simplify the quantification and comparison between WMA and HMA within the same project, this study assumed both aggregate and binder to have the same initial temperature and the aggregate and binders would have the same production temperature, therefore, both aggregate and binder had the same specific heat capacity and their heat energy were equal. The total sum of heat energy ( $Q_t$ ) is the sum of the heat energy of the binder and aggregate. Table 2 shows the conversion coefficients for heat energy reduction percentage of the three fuel types for heating binder and aggregate. These conversion coefficients for specific fuel types (DTI, 2006) are used to determine the volume and each volume is used to determine the percentage reduction of the fuel. Table 3 shows the coefficient values to convert fuel types to CO<sub>2</sub>. The sum of heat energy is linearly related to the CO<sub>2</sub> emission. In this study, the total required heat reduction percentage for HMA and WMA mixture is calculated as follows:

$$\text{Heat reduction (\%)} = \frac{Q(t_{HMA}) - Q(t_{WMA})}{Q(t_{HMA})} \times 100 \quad (4)$$

where  $Q(t_{HMA})$  is the total sum of aggregate and binder heat energy for HMA and  $Q(t_{WMA})$  is the total sum of aggregate and binder the heat energy for WMA. Similarly, the CO<sub>2</sub> reduction is calculated by the ratio of difference in CO<sub>2</sub> emission between HMA and WMA and the CO<sub>2</sub> emission produced by HMA.

### 3.3. Material characterization

#### 3.3.1. Hamburg wheel-tracking device test

Rutting resistance of 150-mm field core was characterized by HWTD test in accordance with AASHTO T324. Field cores were sliced in order to exclude the underlying material and fit into mold. The samples were soaked in water at 50 °C for 2 h prior to testing. Rut depth and number of passes were recorded. HWTD test was stopped when 20-mm rut depth was reached or at the end of 20,000 passes, whichever came first. Neither rut depth at specific pass nor pass at specific rut depth could be used as a single parameter to characterize rutting resistance of varying field cores for comparison purpose. Therefore, rutting resistance index (RRI) that considered both rut depth and number of passes was introduced as follows (Wu et al., 2017, Wen et al., 2016):

$$\text{RRI} = N \times (25.4 - \text{RD}) \quad (5)$$

where, N is number of passes at the completion of test, and RD is measured rut depth at completion of test (mm). A higher RRI indicated a better rutting resistance for an asphalt mixture.

#### 3.3.2. IDT dynamic modulus and creep compliance

Three 100-mm field cores for each material type were subjected to non-destructive testing to obtain indirect tensile (IDT) dynamic modulus at 30 °C with a loading frequency of 0.1 Hz and creep compliance at 30 °C with a loading time of 100s. According to time-

**Table 2**  
Conversion Coefficients for heat energy of different fuel types (DTI, 2006).

Fuel Type	Coefficient	Unit
Diesel	0.006833387	Gallon/MJ
Natural gas	0.9220	Cubic feet/MJ
Coal	0.00004263	Ton/MJ

**Table 3**  
Coefficient to convert fuel types to CO<sub>2</sub> (CRC, 2010).

Fuel Type	Measurement Unit	KgCO <sub>2</sub> /measurement unit
Diesel	Liter	2.639
Natural gas	KWh	0.184
Coal	Ton	2314

temperature superposition principle, lower loading frequency and longer loading time is equivalent to higher temperature for the asphalt mixture. As such, only 30 °C with 0.1 Hz and 30 °C with 100s were used to characterize stiffness at “relatively” high temperature. Four linear variable differential transducers (LVDTs) were mounted on front and back sides of a sliced field core to measure vertical and horizontal deformation, as shown in Fig. 3. Detailed test procedure and calculations of dynamic modulus and creep compliance can be found elsewhere (Shen et al., 2017).

#### 3.3.3. Binder extraction and recovery

After field cores' characterization, the asphalt binders' properties were determined on extracted and recovered asphalt binders from field cores. The extraction procedure followed AASHTO T164, with a solvent of 85% toluene and 15% ethanol by volume. A centrifuge was needed to separate fines from solvent dissolved with extracted asphalt binders. Then the recovery procedure followed AASHTO T170 using the Abson method. By the end of recovery procedure, a flowrate of 900 mL/min is maintained to prompt carbon dioxide throughout recovered asphalt for a 30-min period at 163 °C without seeing a dripping of solvent returned to the flask. It is critical to ensure that solvent is completely out of asphalt binder, otherwise the recovered binder testing results would be misleading.

#### 3.3.4. Performance grading test

High temperature PG test is commonly used to characterize permanent deformation resistance of asphalt binders under in-service high temperature. A 25-mm asphalt binder sample was subjected to a shear stress by controlling shear strain at 10% via a dynamic shear rheometer (DSR), following AASHTO T315. After measuring  $G^*/\sin\delta$  values at two high temperatures, continuous PG was determined as follows:

$$PG_{high} = T_1 + \frac{\log_{10}(2.2) - \log_{10}(G_1)}{\log_{10}(G_2) - \log_{10}(G_1)} \times (T_2 - T_1) \quad (6)$$

where,  $PG_{high}$  is continuous grading high temperature (°C),  $G_1$ ,  $G_2$  are  $G^*/\sin\delta$  measured at temperature  $T_1$  and  $T_2$ , respectively (kPa), and  $T_1$  and  $T_2$  are lower and higher of the two test temperature, respectively.

#### 3.3.5. Multiple stress creep and recovery test

MSCR test was performed in accordance with AASHTO T350 at the pavement high temperature of the specific project according to LTPP Bind software at 98% reliability, which ranges from 46 to 70 °C. One-second creep loading and 9-s rest for ten cycles were conducted, at two respective stress levels of 0.1 kPa and 3.2 kPa. Non-recoverable creep compliance at stress levels of 0.1 kPa ( $J_{nr0.1}$ ) and 3.2 kPa ( $J_{nr3.2}$ ), and percent recovery at 0.1 kPa ( $R_{0.1}$ ) and 3.2 kPa ( $R_{3.2}$ ) were determined as follows. The percent difference ( $J_{nr\text{diff}}$ ) was also calculated to characterize stress sensitivity of asphalt binder.

$$J_{nr0.1} = \frac{\varepsilon_{10}}{0.1} \quad (7)$$



Fig. 3. IDT dynamic modulus and creep compliance measurement setup (Shen et al., 2017).

$$J_{nr3.2} = \frac{\epsilon_{10}}{3.2} \quad (8)$$

$$J_{nr\text{diff}} = \frac{J_{nr3.2} - J_{nr0.1}}{J_{nr0.1}} \times 100 \quad (9)$$

$$R_{0.1} = \frac{\epsilon_{10} - \epsilon_1}{\epsilon_1} \times 100 \quad (10)$$

$$R_{3.2} = \frac{\epsilon_{10} - \epsilon_1}{\epsilon_1} \times 100 \quad (11)$$

where,  $\epsilon_1$  denotes the strain at the end of creep portion of each cycle; and  $\epsilon_{10}$  denotes the strain at the end of recovery portion of each cycle. Previous study indicated that  $R_{3.2}$  was determined as a significant determinant for permanent deformation resistance (rutting resistance) performance (Shen et al., 2017).

### 3.3.6. Monotonic shear strength test

Unlike PG and MSCR tests, monotonic shear test using a DSR was to shear fracture asphalt by controlling shear rate at 20 °C (Shen et al., 2017; Wu, 2018). The sample size of recovered asphalt binder for this test was 4-mm, and the shear rate used in this study was 0.3 s<sup>-1</sup>. A shear stress versus shear strain curve was obtained, and the peak shear stress indicated the maximum shearing capacity of asphalt binders was able to sustain. At the peak stress, the corresponding shear strain was defined as failure strain. Higher failure strain resulted in a higher ductility (Wu, 2018). Fracture energy, also called yield energy, can be also determined by the area of the curve up to peak stress.

## 4. Results and discussions

### 4.1. Extracted binders' PG test results

Asphalt binder with increased high temperature PG exhibits a more resistance to permanent deformation. Fig. 4 compares PG of the extracted WMA binder with that of the extracted HMA binder, using a box plot where the first Quartile, median, and third Quartile are presented. Generally, the HMA and WMA binders exhibited comparable PG, with a median value of approximately zero, although there were some variations between a few HMA and WMA binder comparison pairs. In addition, current Superpave PG systems use 6 °C to determine different grades for asphalt binder. The majority of comparison pairs of HMA and WMA binder were less than 6 °C. This is to say, the WMA binder exhibited similar resistance to permanent deformation as the HMA binder.

### 4.2. MSCR test results

AASHTO M322 specified four categories of traffic: Standard, Heavy, Very Heavy, and Extremely heavy, that asphalt binder was able to sustain each traffic level based on  $J_{nr3.2}$  value. In this study, 53 out of 83 asphalt binders were able to sustain "Extremely heavy" traffic, whose  $J_{nr3.2}$  value was less than 0.5 kPa<sup>-1</sup>; 119 out of 83 binders can sustain "Very Heavy" traffic, whose  $J_{nr3.2}$  value is less than 1 kPa<sup>-1</sup> but more than 0.5 kPa<sup>-1</sup>. Only 11 out of 83 binders were able to sustain "Heavy" traffic, whose  $J_{nr3.2}$  value was more than 1 kPa<sup>-1</sup> but less than 2 kPa<sup>-1</sup>. Detailed data results refer to Shen et al. (2017).

Fig. 5a presents a box plot of  $J_{nr3.2}$  value comparison between HMA and WMA binders. As seen, the median value was close to zero and the difference in  $J_{nr3.2}$  value between HMA and WMA binder was marginal. This also indicated that after long-term field aging, the permanent deformation resistance of the WMA binder was comparable as that of the HMA binder, which is further confirmed by Fig. 5b where the  $R_{3.2}$  value is compared. Again, the HMA and WMA binder in general showed comparable recovery property, indicating a comparable permanent deformation resistance. Lower  $J_{nr3.2}$  value and higher  $R_{3.2}$  resulted in better resistance to permanent deformation.

### 4.3. Relationship between $J_{nr3.2}$ and $R_{3.2}$

Fig. 6 plots the relationship between  $J_{nr3.2}$  and  $R_{3.2}$ . The red line is also plotted based on the formula given according to AASHTO M322, which can be used as indicator of the presence of

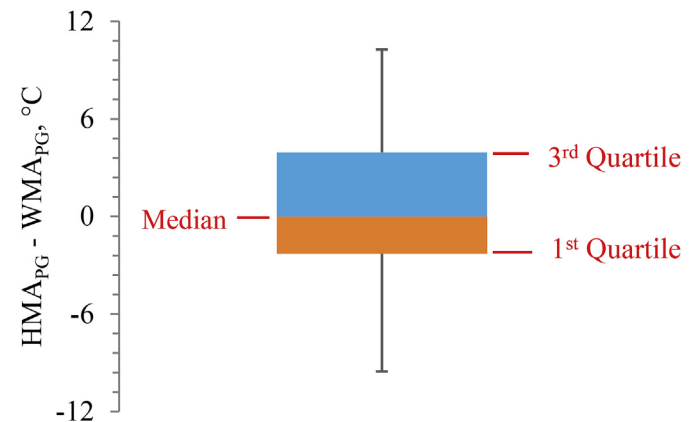


Fig. 4. High temperature PG comparison between HMA and WMA binders.

elastomeric polymer in asphalt binders. The dot above red line indicated an existence of polymer in this binder, while the dot below the red line indicated failing percent recovery and none of polymers. According to Table 1, 19 out of 28 projects (55 out of 83 asphalt binders) used polymer modified binders, however, this plot indicated that only 6 projects (15 asphalt binders) exhibited polymer binders evidenced by the dots above red lines. These projects were WA I-90, LA 3121, NV, TX SH 71, MT I-15 and LA US 61 projects, which appeared to be polymer-survived. Most of these “polymer-survived” projects were relatively young with less than 2 years’ old. For those projects used polymer modified asphalt but did not survive after long-term field aging, polymer network in those binders could have been damaged and deteriorated, which was also observed by Islam et al. (2016).

It was also noted that those 15 “polymer-survived” asphalt binders included both HMA and WMA binders. In other words, regardless of HMA and WMA types, polymer was affected by field aging rather than WMA additives. The long-term field aged polymer modified asphalt binders for WMA and HMA were comparable. However, more research is needed to understand the interaction between WMA additives and different polymers from multiscale analysis.

#### 4.4. Field cores mixtures test results

Fig. 7(a) to 7(c) present the overall HMA and WMA field cores comparison with respect to dynamic modulus, creep compliance,

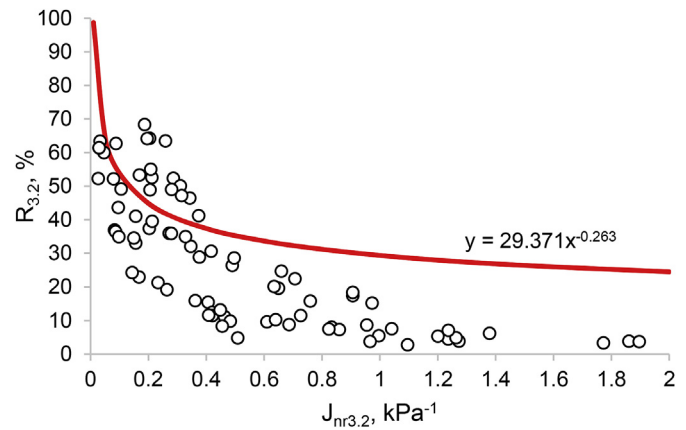


Fig. 6. Relationship between  $J_{nr3.2}$  and  $R_{3.2}$ .

and rutting resistance index respectively. Based on the median value, HMA field cores had slightly higher dynamic modulus, lower creep compliance, and higher rutting resistance index than WMA field cores. Both dynamic modulus and creep compliances were measured at 30 °C, while the rutting resistance index were obtained from HWT test at 50 °C. A large range of difference indicated by error bar was attributed to various material types and projects. Overall, the HMA and WMAs’ difference was marginal.

#### 4.5. Correlation of binders’ properties and asphalt mixtures’ properties

Asphalt binders’ rheological properties contribute significantly to asphalt pavement’s permanent deformation resistance (Szydło and Mackiewicz, 2005). To characterize the correlation between binders’ properties to asphalt mixtures’ properties, correlation coefficient was used. Since the properties for binders and mixtures were achieved in a similar test conditions and consisted into pair  $(x_1, y_1), (x_2, y_2), \dots, (x_n, y_n)$ , where  $x_i$  is one observation of binder property and  $y_i$  is one observation of mixture property, correlation coefficient ( $r$ ) was determined as follows (Devore, 2010):

$$r = \frac{\sum_{i=1}^n (x_i - \bar{x})(y_i - \bar{y})}{\sqrt{\sum (x_i - \bar{x})^2} \sqrt{\sum (y_i - \bar{y})^2}} \quad (12)$$

where,  $x_i$  is binder property,  $y_i$  is mixture property, and  $\bar{x}$  and  $\bar{y}$  denote average binder property and average mixture property, respectively.

Table 4 presents the correlation coefficients between asphalt binders’ properties and asphalt mixtures’ properties. “+” and “-” denote positive and negative correlation, respectively. The closer the value of  $r$  to 1 or -1, indicating the stronger positive or negative correlation. Weak correlation may occur due to the effect of aggregate and gradation, therefore, based on literature and previous studies on correlation between binders and mixtures (Behnood et al., 2016; Devore, 2010), this study used the following category to characterize the correlation: strong correlation (either  $r \geq 0.8$  or  $r \leq -0.8$ ), moderate correlation (either  $-0.5 \leq r < -0.8$  or  $0.5 \leq r < 0.8$ ), having a general trend (either  $-0.2 < r < -0.5$ , or  $0.2 < r < 0.5$ ), and weak correlation ( $-0.2 \leq r \leq 0.2$ ).

As seen in Table 4, only high temperature PG had fairly moderate correlation with all mixtures’ properties. A higher PG value correlated well with a higher dynamic modulus, lower creep compliance, and higher rutting resistance index. None of parameters from MSCR test had a good correlation with dynamic modulus and creep

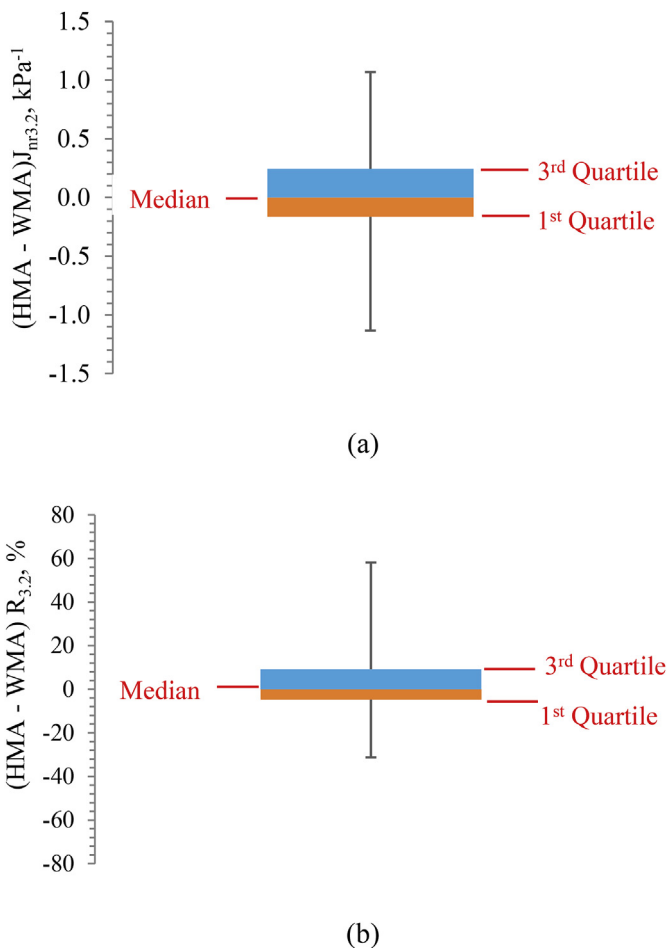


Fig. 5. Difference between HMA and WMA binders (a)  $J_{nr3.2}$  and (b)  $R_{3.2}$ .

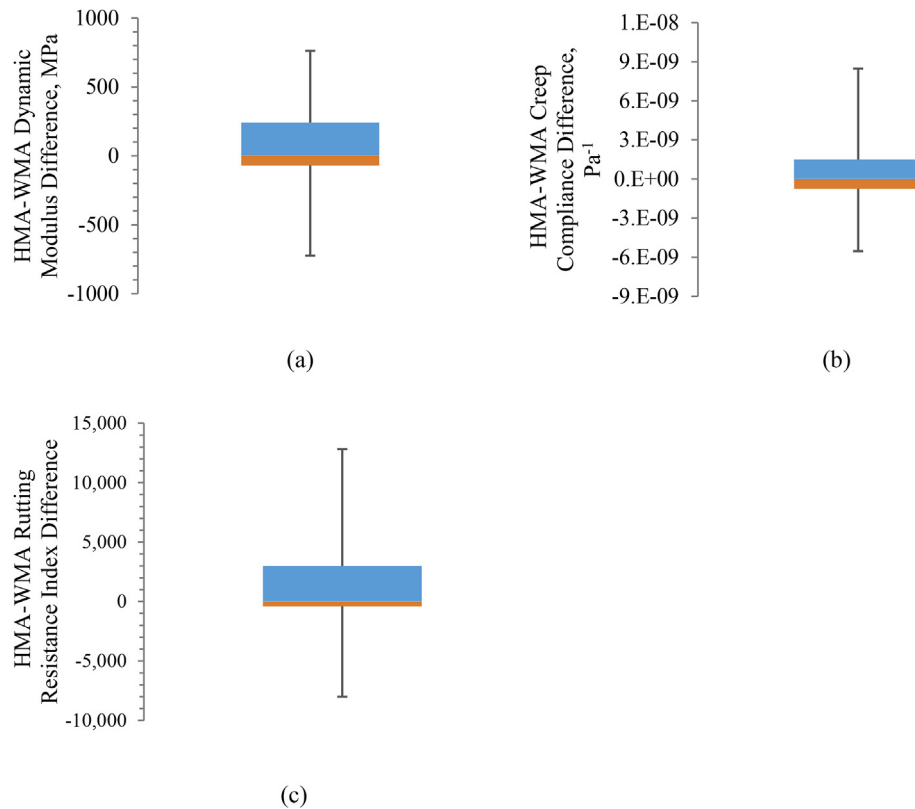


Fig. 7. Box plots of difference between HMA and WMA field cores with respect to: (a) dynamic modulus, (b) creep compliance, and (c) rutting resistance index.

compliance, however, peak stress from DSR monotonic test had moderate correlation with them. Percent recovery showed a general trend with rutting resistance index of mixture. A higher percent recovery of asphalt binder exhibited a higher rutting resistance index. Overall, the results suggested that PG test and percent recovery were able to indicate permanent deformation resistance of long-term field aged asphalt mixtures.

#### 4.6. Correlation among binders' properties

Additional analysis on correlation among binder properties was conducted, and the correlation results are shown in Table 5. Parameters from the same test had a very strong correlation, such as  $J_{nr0.1}$  versus  $J_{nr3.2}$ , and  $R_{0.1}$  versus  $R_{3.2}$ . Stress sensitivity is calculated by the difference percentage in non-recoverable creep compliance at 0.1 kPa and 3.2 kPa, and it was found that for the majority of long-term aged asphalt binders, the stress sensitivity value was way lower than 75%, and  $J_{nr3.2}$  was less than  $0.5 \text{ kPa}^{-1}$ , and therefore asphalt binders were designated as "E" (extremely high traffic

level) according to AASHTO M332. This was to imply that field aging had significantly improved asphalt binders' long-term rutting resistance. Failure strain from monotonic test had a good correlation with percent recovery from MSCR test, both of which indicated binders' resistance to permanent deformation. Shear strength correlated very well with PG that the higher shear strength, the higher PG, and both values indicated binders' resistance to permanent deformation.

#### 4.7. Environmental impact analysis

The reduced production temperature of WMA technology contributes for the reduction heat energy and therefore reduction of  $\text{CO}_2$  emissions. Table 6 shows the  $\text{CO}_2$  reduction percentage for each project that compares WMA technology with HMA, in terms of three main fuel types: diesel, gas and coal.

According to Table 6, the use of WMA technologies can have an important impact on the heating energy of fuel types and in the reduction of  $\text{CO}_2$ . Fig. 8 presents the box plot for the reduction in

Table 4  
Correlation coefficients of properties between asphalt binders and mixtures.

Correlation Coefficient		Mixtures' Property		
		Dynamic Modulus, 30 °C, 0.1Hz, MPa	Creep Compliance, 30 °C, 100s, 1/Pa	Rutting Resistance Index, 50 °C
<b>Binders' Property</b>	$PG_{high}$	+0.68	-0.69	+0.47
	$J_{nr0.1}$ , 1/kPa	-0.03	+0.19	-0.09
	$J_{nr3.2}$ , 1/kPa	-0.004	+0.16	-0.04
	$J_{nr diff}$ , %	+0.18	-0.21	+0.29
	$R_{0.1}$ , %	+0.09	-0.41	+0.49
	$R_{3.2}$ , %	+0.05	-0.37	+0.42
	Peak Stress, kPa	+0.54	-0.44	+0.07
	Failure Strain	-0.24	-0.08	+0.24

**Table 5**  
Correlation coefficients of properties among asphalt binders.

<i>r</i>	$PG_{high}$	$J_{nr0.1}$	$J_{nr3.2}$	$J_{nr diff}$	$R_{0.1}$	$R_{3.2}$	Shear Strength	Failure Strain
$PG_{high}$	1.00							
$J_{nr0.1}$	-0.39	1.00						
$J_{nr3.2}$	-0.35	1.00	1.00					
$J_{nr diff}$	0.05	0.23	0.25	1.00				
$R_{0.1}$	0.45	-0.73	-0.71	-0.02	1.00			
$R_{3.2}$	0.43	-0.76	-0.75	-0.11	0.99	1.00		
Shear Strength	0.75	-0.22	-0.21	-0.19	0.10	0.13	1.00	
Failure Strain	-0.14	-0.25	-0.25	-0.14	0.60	0.61	-0.29	1.00

CO<sub>2</sub>. Depending on the WMA type, the CO<sub>2</sub> reduction can be as high as 89.09% and as low as 42.79%. The highest CO<sub>2</sub> reduction was recorded while comparing HMA to Advera in TN SR 46 project. On average, the CO<sub>2</sub> emission can be reduced to 66.89% by using WMA technologies. All three fuel types have the same median, maximum and minimum values which means that the heat energy does not affect differently fuel types and therefore the CO<sub>2</sub> reduction remains the same for three fuel types calculation.

## 5. Conclusions

This study evaluated the environmental impacts of WMA

technologies as compared to HMA for 28 field projects across U.S., as well as permanent deformation resistance for extracted HMA and WMA binders and asphalt mixtures based on 83 field samples. The outcome of this study would be helpful to select appropriate testing and properties to characterize long-term permanent deformation resistance for various asphalt materials. The major findings in this study are summarized as follows:

- Depending on the WMA type, the CO<sub>2</sub> reduction ranged from 89.09% to 42.79%. On average, the CO<sub>2</sub> emission could be reduced to 66.89% by using WMA technologies.

**Table 6**  
CO<sub>2</sub> reduction (%) of WMA technology as compared to HMA in each project.

Project	HMA Production Temp., °C	WMA		CO <sub>2</sub> reduction (%)		
		Type	Production Temp., °C	Diesel	Gas	Coal
MD 925	177	Sasobit	154	50.16	50.16	50.16
MO Hall St.	160	Sasobit	116	81.78	81.78	81.78
		Evotherm ET	107	87.75	87.75	87.75
		Asphamin	135	58.73	58.73	58.73
		Evotherm DAT	143	43.57	43.57	43.57
MO Rte. CC	160	Evotherm 3G	129	51.86	51.86	51.86
MN TH 169	149	Sasobit	127	70.45	70.45	70.45
OH SR 541	160	Evotherm ET	113	83.98	83.98	83.98
		Asphamin	118	79.34	79.34	79.34
		LEA	129	60.21	60.21	60.21
		Gencor	127	64.49	64.49	64.49
VA I-66	158	Astec DBG	142	42.79	42.79	42.79
IL 147	149	Astec DBG	132	46.20	46.20	46.20
PA SR 2006	154	Sasobit	129	60.21	60.21	60.21
		Advera	127	64.49	64.49	64.49
		Evotherm DAT	116	70.79	70.79	70.79
SC US 178	146	Evotherm DAT	121	86.02	86.02	86.02
TN SR 46	177	Advera	116	89.09	89.09	89.09
		Astec DBG	127	69.21	69.21	69.21
		Sasobit	116	84.73	84.73	84.73
		Evotherm DAT	116	84.73	84.73	84.73
TX FM 324	166	Rediset	116	84.73	84.73	84.73
		Advera	116	84.73	84.73	84.73
		Evotherm 3G-1	132	71.55	71.55	71.55
		Evotherm 3G-2	144	54.84	54.84	54.84
LA 3121	168	Sasobit	136	64.67	64.67	64.67
WA I-90	166	Sasobit	124	68.40	68.40	68.40
CO IH 70	154	Evotherm DAT	121	71.96	71.96	71.96
		Advera	124	68.40	68.40	68.40
		Evotherm DAT	135	65.42	65.42	65.42
NE US 14	166	Evotherm DAT	135	65.42	65.42	65.42
NV	166	Ultrafoam	135	65.42	65.42	65.42
TX SH 251	154	Astec DBG	132	55.53	55.53	55.53
TX SH 71	166	Evotherm DAT	116	84.73	84.73	84.73
CA HVS 3a	160	Gencor	140	50.09	50.09	50.09
		Evotherm DAT	120	77.76	77.76	77.76
		Cecabase	130	66.13	66.13	66.13
CA HVS 3b	168	Sasobit	149	47.12	47.12	47.12
		Advera	146	52.06	52.06	52.06
		Astec DBG	146	52.06	52.06	52.06
		Rediset	141	60.83	60.83	60.83

Note: Some projects' data are missing due to inability to collect the production temperatures.

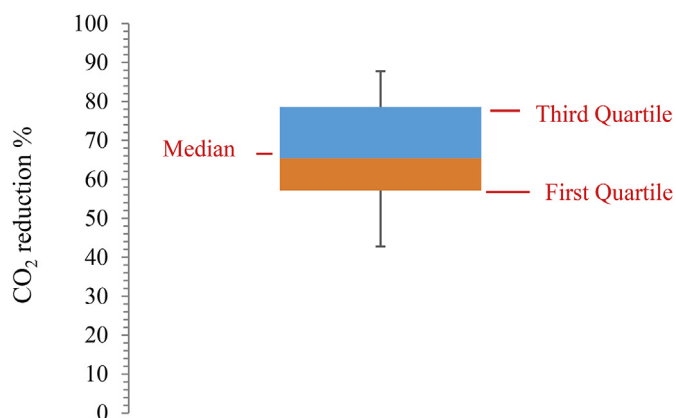


**Fig. 8.** Box plot for CO<sub>2</sub> reduction (%).

Note: The orange box denotes the first Quartile and the blue box denotes the third Quartile. (For interpretation of the references to colour in this figure legend, the reader is referred to the Web version of this article.)

- The WMA binder exhibited similar resistance to permanent deformation as the HMA binder after long-term field aging. The use of WMA could help asphalt industry to achieve environmental benefits without compromising long-term rutting resistance.
- The plot of non-recoverable creep compliance and percent recovery at 3.2 kPa helped identify the existence of polymer in the asphalt binder. Long-term field aging may deteriorate and damage polymer network in the asphalt binders. The long-term field aged polymer modified asphalt binders for WMA and HMA were comparable, which ensured a confident use of WMA technology.
- Field cores characterization indicated that HMA and WMAs' differences in dynamic modulus, creep compliance, and rutting resistance were marginal.
- For all HMA and WMA binders tested at high temperature, binders' PG correlated strongly with properties of mixtures. A higher percent recovery of asphalt binder exhibited a higher rutting resistance index of asphalt mixture.
- Correlation among asphalt binders' properties from MSCR test results showed that field aging has significantly improved asphalt binders' long-term rutting resistance.
- Overall, the environmental impact analysis and long-term field rutting results provided a confidence in adopting WMA technologies.

### CRedit authorship contribution statement

**Shenghua Wu:** Conceptualization, Data curation, Formal analysis, Writing - original draft, Writing - review & editing. **Omar Tahr:** Data curation, Formal analysis, Writing - original draft, Writing - review & editing. **Shihui Shen:** Conceptualization, Formal analysis, Writing - original draft, Writing - review & editing. **Weiguang Zhang:** Conceptualization, Data curation, Formal analysis, Writing - original draft, Writing - review & editing. **Balasingam Muhunthan:** Conceptualization, Writing - original draft, Writing - review & editing.

### Declaration of competing interest

The authors declare that they have no known competing financial interests or personal relationships that could have appeared to influence the work reported in this paper.

### Acknowledgement

The authors would like to acknowledge National Cooperative Highway Research Program (NCHRP) 9–49A project to sponsor this study. The state departments of transportation (DOTs) who helped with field coordination, federal highway agency, industry contractors, university partners, as well as many graduate and undergraduate students for their helpful assistances are also greatly appreciated.

### References

- Blankendaal, T., Schuur, P., Voordij, H., 2014. Reducing the environmental impact of concrete and asphalt: a scenario approach. *J. Clean. Prod.* 66, 27–36.
- Behnood, A., Shah, A., McDaniel, R.S., Beeson, M., Olek, J., 2016. High-temperature properties of asphalt binders: comparison of multiple stress creep recovery and performance grading systems. *Transport. Res. Rec.: Journal of the Transportation Research Board* 2574, 131–143.
- CRC energy efficiency scheme order. [www.decc.gov.uk](http://www.decc.gov.uk), 2010.
- D'Angelo, J., Kluttz, R., Dongré, R., Stephens, K., Zanzotto, L., 2007. Revision of the superpave high temperature binder specification: the multiple stress creep recovery test. *Journal of the Association of Asphalt Paving Technologists* 76, 123–162.
- Devore, J.L., 2010. *Probability and Statistics for Engineering and the Sciences*, eighth ed. Brooks/Cole, Boston.
- Dongré, R., D'Angelo, J., Reinke, G., 2004. New criterion for superpave high-temperature binder specification. *Transport. Res. Rec.: Journal of the Transportation Research Board* (1875), 22–32.
- Domingos, M.D.I., Faxina, A.L., Bernucci, L., 2017. Characterization of the rutting potential of modified asphalt binders and its correlation with the mixture's rut resistance. *Construct. Build. Mater.* 144, 207–213.
- DTI, 2006. *Digest of United Kingdom Energy Statistics 2006*. Department of Trade and Industry.
- Gandhi, T., Akisetty, C., Amirhanian, S., 2009. Laboratory evaluation of warm asphalt binder aging characteristics. *Int. J. Pavement Eng.* 10, 353–359.
- Hamzah, M.O., Jamshidi, A., Shahadan, Z., 2010. Evaluation of the potential of sasobit® to reduce required heat energy and CO<sub>2</sub> emission in the asphalt industry. *J. Clean. Prod.* 18, 1859–1865. <https://doi.org/10.1016/j.jclepro.2010.08.002>.
- Islam, R.M., King, W., Wasiuddin, N.M., 2016. Correlating long-term chip seals performance and rheological properties of aged asphalt binders. *J. Mater. Civ. Eng.* 28 [https://doi.org/10.1061/\(ASCE\)MT.1943-5533.0001487](https://doi.org/10.1061/(ASCE)MT.1943-5533.0001487).
- Kim, Y.R., Castorena, C., Elwardany, M., Rad, F.Y., Underwood, S., Gundha, A., Gudipudi, P., Farrar, M.J., Glaser, R.R., 2017. Long-Term Aging of Asphalt Mixtures for Performance Testing and Prediction. NCHRP Research Report 871. Transportation Research Board, Washington, D.C. <https://doi.org/10.17226/24959>.
- Ramadan, S., Gundla, A., Zalgout, A., Underwood, B.S., Kaloush, K.E., 2019. Relationship between asphalt binder parameters and asphalt mixture rutting. *Transport. Res. Rec.: Journal of the Transportation Research Board* 2673, 431–446.
- Shen, S., Wu, S., Zhang, W., Mohammad, L.N., Muhunthan, B., 2017. Performance of WMA technologies: stage II – long-term field performance. NCHRP Report 843. <https://doi.org/10.17226/24708>.
- Shenoy, A., Stuart, K., Mogawer, W., 2003. Do asphalt mixtures correlate better with mastics or binders in evaluating permanent deformation. *Transport. Res. Rec.: Journal of the Transportation Research Board* 1829, 16–25.
- Soleymani, H.R., Zhai, H., Bahia, H., 2004. Role of modified binders in rheology and damage resistance behavior of asphalt mixtures. *Transport. Res. Rec.: Journal of the Transportation Research Board* 1875, 70–79.
- Szydio, A., Mackiewicz, P., 2005. Asphalt mixes deformation sensitivity to change in rheological parameters. *J. Mater. Civ. Eng.* 17, 1–9.
- Tatari, O., Nazzal, M., Kucukvar, M., 2012. Comparative sustainability assessment of warm-mix asphalt: a thermodynamic based hybrid life cycle analysis. *Resour. Conserv. Recycl.* 58 (2012), 18–24.
- Waples, D.W., Waples, J.S., 2004. A review and evaluation of specific heat capacities of rocks, minerals, and surface fluids, part 1: mineral and non porous rocks. *J. Nat. Resour. Researches* 13 (2), 97–122.
- Wen, H., Wu, S., Mohammad, L.N., Zhang, W., Shen, S., Faheem, A., 2016. Long-term field rutting and moisture susceptibility performance of warm-mix asphalt pavement. *Transport. Res. Rec.: Journal of the Transportation Research Board* 2575, 103–112.
- Wu, S., Al-Qadi, I.L., Lippert, D.L., Ozer, H., Espinoza-Luque, A.F., Safi, F.R., 2017. early-age performance characterization of hot-mix asphalt overlay with varying amounts of asphalt binder replacement. *Construct. Build. Mater.* 153, 294–306.
- Wu, S., 2018. Characterization of ductility of field-aged petroleum asphalt. *Petrol. Sci. Technol.* 36, 696–703.
- Wu, S., Zhang, W., Shen, S., Muhunthan, B., 2019. Field performance of foaming warm mix asphalt pavement. *Transport. Res. Rec.: Journal of the Transportation Research Board* 2673, 281–294.